ANTIFUNGAL MULBERRY PAPERS MODIFIED WITH MICROCLUSTERS OF PYRAMIDAL ZINC OXIDE

CHAT PHOLNAK, NUSROFAH LATTE, CHITNARONG SIRISATHITKUL,[*] MONTHON LERTWORAPREECHA[**] and SUMETHA SUWANBOON[***]

Department of Physics, Faculty of Science, Thaksin University, Phatthalung 93210, Thailand
[*]Molecular Technology Research Unit, School of Science, Walailak University, Nakhon Si Thammarat 80160, Thailand
[**]Department of Biology, Faculty of Science, Thaksin University, Phatthalung 93210, Thailand
[***]Department of Materials Science and Technology, Faculty of Science, Prince of Songkla University, Songkhla 90112, Thailand
✉ *Corresponding author: Chitnarong Sirisathitkul, chitnarong.siri@gmail.com*

The calcination of zinc nitrate hexahydrate ($Zn(NO_3)_2{\cdot}6H_2O$) crystals was demonstrated as a facile route for preparing single-phase zinc oxide (ZnO) microclusters composed of pyramids around 15 μm in size. Their antifungal property was tested on mulberry papers made from the woody stem of tube sedge (*Lepironia articurata*). The papers coated by 2-12 mg/mL of ZnO dispersion exhibited a resistance to *Aspergillus niger* when subjected to the fungus for up to 15 days. The inhibition was attributed to the photocatalytic activity of the ZnO microclusters, which is not sensitive to the calcination temperature from 600 to 800 °C. This finding is beneficial for the manufacture of antifungal handicraft products from mulberry papers and of local bulrush basketry from tube sedge.

Keywords: zinc oxide, antifungal properties, optical properties, mulberry paper, tube sedge

INTRODUCTION

Tube sedge (*Lepironia articurata* (*Retz.*) *Domin*) has a woody stem, which can be used for manufacturing handicrafts.[1] Mulberry papers from tube sedge are also commercialized for decorating and packaging proposes. Such specialty papers are acid-free and textured due to natural long fibers. In addition to their appearance, these products are valued for the manual manufacturing process, utilizing local plant residues as source materials. For the Talay Noi community in the south of Thailand, bulrush basketry and other products from tube sedge are reputable and have become an important source of local income. However, bulrush basketry and mulberry papers easily deteriorate from fungal growth because of their hydrophilic and highly porous organic nature. The damages caused by fungal attacks lead to considerable losses during the postharvest handling process under the warm and humid climate. It is, therefore, important to explore antifungal agents that are more effective and environmentally friendly than conventional fungicides. For example, lime oil and heat treatment at 70 °C inhibited the growth of *Aspergillus niger*, a common airborne fungus, on the surface of sedge for up to 18 weeks.[2]

Zinc oxide (ZnO) is a promising functional material for many emerging applications, in which its electrical, optical and chemical properties can all be exploited. Moreover, ZnO is known for its antimicrobial properties. Several works on its antibacterial activity have been reported and extensively reviewed.[3,4] Applications are extended to antibacterial papers coated with ZnO or its composites.[5,6] On the other hand, a much smaller number of works involve the antifungal activity of ZnO. Examples include fungi such as *Botrytis cinerea*,[7] *Penicillium expansum*,[7] *Candida albicans*,[8] *Rhizopus stolonifer*,[8,9] *Aspergillus flavus*,[9] *Aspergillus nidulans*,[9] *Trichoderma harzianum*,[9] *Fusarium sp*.,[10] *Aspergillus brasiliensis*,[11] *Trichoderma reesei*[12] and *A. niger*.[12] The potential applications have been demonstrated on paintings,[12] wood boards[13] and writing papers.[14]

In this study, mulberry papers prepared from locally available tube sedge were coated with ZnO and the antifungal activity of the coated samples was investigated against *A. niger*. The ZnO was obtained directly by single-step calcination.

EXPERIMENTAL

Five samples were prepared by calcining 20 g of $Zn(NO_3)_2{\cdot}6H_2O$ (98%, Sigma-Aldrich) at 400 °C, 500 °C, 600 °C, 700 °C and 800 °C in a programmable muffle furnace (Chavachote, Thailand). Under ambient conditions, the furnace was heated to a calcination temperature with a heating rate of 5 °C/min and maintained at this temperature for 3 h. After cooling down to room temperature, white mellow powders were collected and then further characterized.

The phase and morphology were characterized, respectively, by X-ray diffractometry (XRD; Phillips X'pert MPD), using Cu-K_α radiation, and scanning electron microscopy (SEM; FEI Quanta 400), using an accelerating voltage of 25 kV. Optical properties were characterized by UV-Vis spectrophotometry (Shimadzu UV-2450) from 200 to 800 nm and photoluminescence (PL) spectrophotometry (PerkinElmer LS/55) from 250 to 800 nm.

The antifungal activity against *A. niger* was tested by the standard inhibitory diffusion assay. The conidia spore suspension of the fungus was adjusted to approximately 10^5 conidia spore/mL by normal saline (0.85%). On the testing date, a hundred μL of adjusted spore was spread on potato dextrose agar (PDA) (Himedi, India). To test the antifungal efficacy of the ZnO coating, four square samples (3×3 cm^2) were cut from a sheet of mulberry paper made from underground stems of the tube sedge. Each paper was coated with ultrasonically treated ZnO dispersion with varying concentrations (0, 2, 6, 12 mg/mL), then dried in a class II biosafety cabinet for 30 min and finally applied onto the PDA plate. The pathogenic fungal growth on each paper was monitored by direct optical observation after 1, 5, 10 and 15 days of inoculation.

RESULTS AND DISCUSSION

Morphology and phase

After calcining at 400-800 °C, all the XRD patterns in Figure 1 exhibit sharp peaks at 36.2°, 31.7°, 34.3°, 47.5°, 56.5°, 59.6°, 62.8°, 66.3°, 67.8° and 69.0°, which are assigned to the wurtzite ZnO with a space group of P63mc (JCPDF No.01-079-2205). The ZnO is formed without any impurity phase during the calcination process according to the following reaction:

$$Zn(NO_3)_2{\cdot}6H_2O(s) \xrightarrow{\Delta T} Zn(NO_3)_2{\cdot}6H_2O(l) \rightarrow ZnO(s) + 6H_2O(g) + 2NO_2(g) + \frac{1}{2}O_2(g) \quad (1)$$

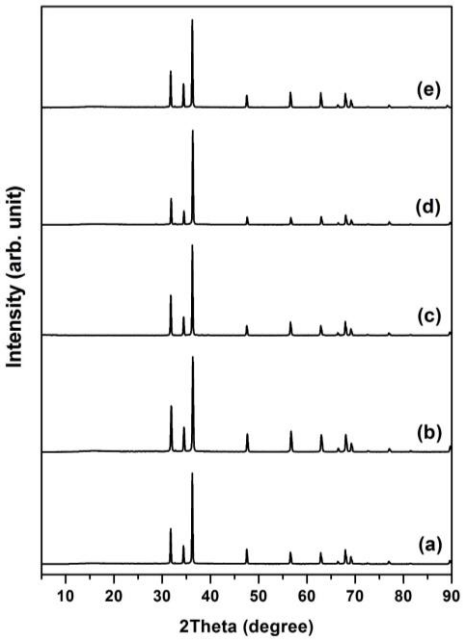

Figure 1: XRD patterns of powders calcined at 400 °C, 500 °C, 600 °C, 700 °C and 800 °C

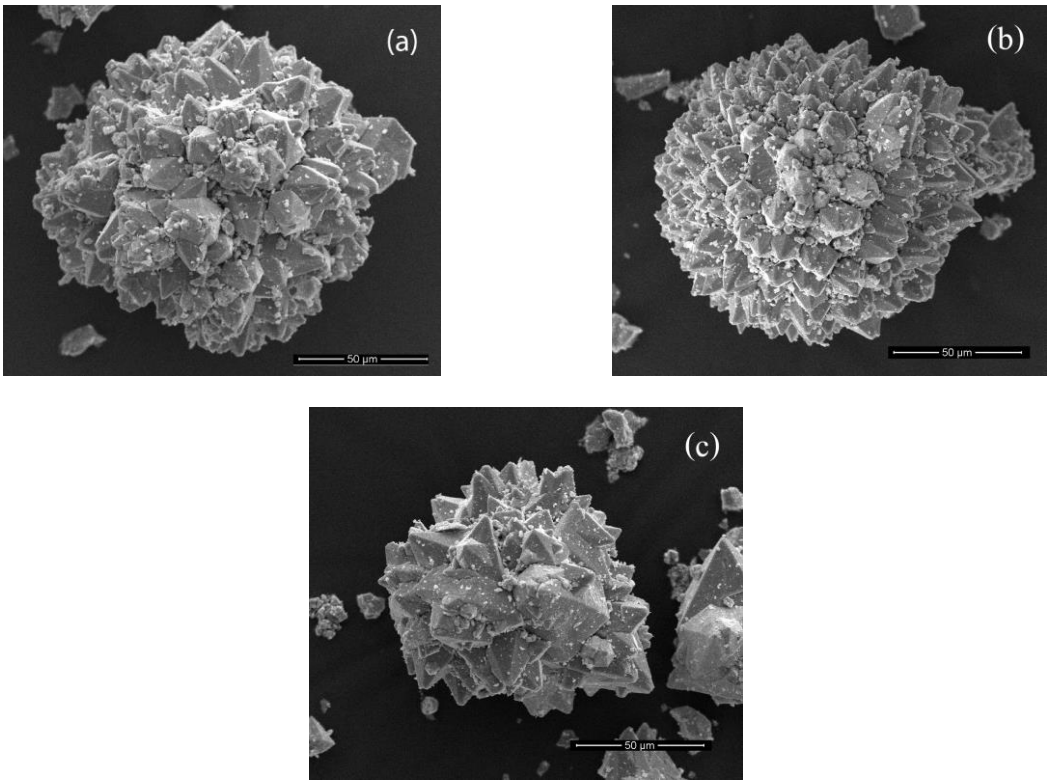

Figure 2: SEM micrographs of ZnO obtained by calcination at (a) 600 °C, (b) 700°C and (c) 800 °C

Similar to the phase, the morphology is not affected by the variation in calcination temperature from 600 to 800 °C. SEM images in Figure 2 show the ZnO microclusters approximately 100 μm in size. These clusters are composed of hexagonal pyramids of similar sizes – around 15 μm. By calcining at 600 and 700 °C (Fig. 2(a) and 2(b)), ZnO clusters are formed by the aggregation of a large number of hexagonal based pyramids oriented in the manner of three-dimensional microstructures. As seen in Figure 2(c), the morphology is still preserved at 800 °C, but the aggregation is slightly decreased.

According to previous suggestions on the growth mechanism of aggregated ZnO,[15,16] hexagonal pyramids form a fundamental unit of ZnO polyhedron by aggregating into three-dimensional microstructures. The characteristic shape of pyramids, with six triangular faces and a sharp tip, was obtained by direct pyrolysis of the $Zn(NO_3)_2 \cdot 6H_2O$ precursor.[17] The initial melting leads to the deliquescence of the precursor and the oriented growth during the calcination. Subsequently, the growth and aggregation of hexagonal pyramids occur with the base of hexagonal pyramids forming the center of ZnO microclusters.[15] Normally, ZnO is a polar crystal with a characteristic preference for the polar axis growth, *i.e.* along the [0001] direction or c-axis. In the hydrothermal process, the continued growth of the units on the [0001] facet generally results in the formation of hexagonal ZnO nanorods.[18] Due to the attachment of nitrate ions onto the facet, the nitrate ions adsorb onto the polar plane. The growth of ZnO is retarded and a sharp end at the c-axis is formed, resulting in hexagonal pyramids.[19]

Optical properties

As has been reported in the literature, the growth and properties of ZnO are sensitive to the process parameters. Examples include reagent concentration and synthesis time for the sonochemical method[20] and electrodeposition.[21] It is notable that the morphology and optical properties are not dependent on the conditions used in this work. The UV-Vis spectra presented in Figure 3 and the PL spectra in Figure 4 exhibiting three varying calcination temperatures are almost identical. For all the UV-Vis spectra, the UV absorption from 200 to 400 nm is substantial, but sharply drops in the visible regime.

All the PL spectra exhibit UV-B, UV-A, violet and red emission peaks. The small and broad UV peak centered at 318 nm is due to the near band edge emission, whereas the major UV peak around 390 nm corresponds to the recombination of free excitons.[22] For the visible regime, the sharp violet peak at 412 nm is associated with the transition from the shallow defect level to the valence band. Finally, the broad band from 500 nm to 800 nm is assigned to the deep level emission from the defects in which the high intensity is attributed to high density of ZnO defects.[23] Interestingly, these optical properties are comparable for different morphologies of ZnO.[20]

Antifungal properties

The antifungal activity was assessed by the ability of *A. niger* to grow on the differently treated samples. The uncoated mulberry paper in Figure 5 has several colonies of *A. niger* grown on its surface. On the other hand, the growth of *A. niger* on the mulberry papers coated with ZnO is inhibited and only limited fungal spores are observed on the samples. The diffusion method emphasizes the increased effectiveness of the ZnO coating with concentrations of up to 12 mg/mL, by the expanding clear zone. *A. niger* has increasingly grown on the uncoated sample during up to 15 days, while the surfaces of the coated papers remained free from fungal attack.

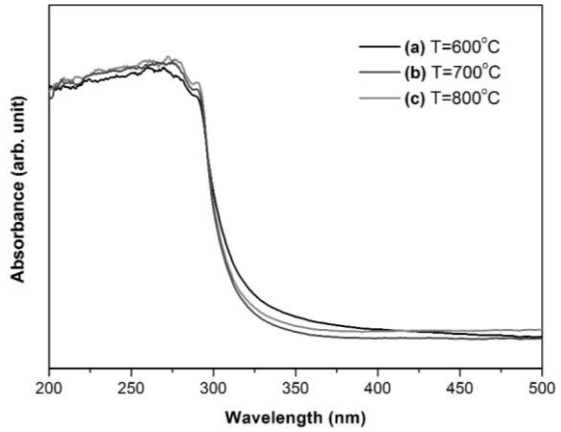

Figure 3: Room temperature UV-Vis spectra of ZnO obtained by calcination at (a) 600 °C, (b) 700 °C and (c) 800 °C

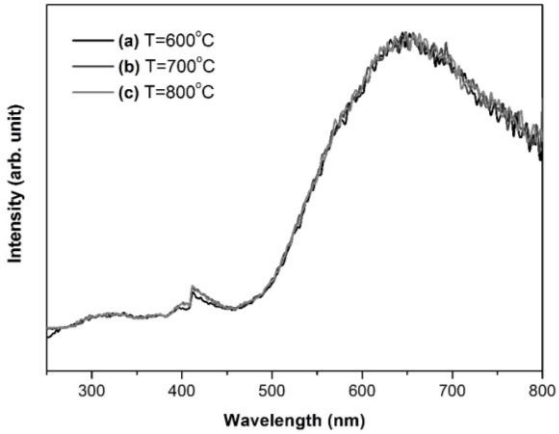

Figure 4: Room temperature PL spectra of ZnO obtained by calcination at (a) 600 °C, (b) 700 °C and (c) 800 °C

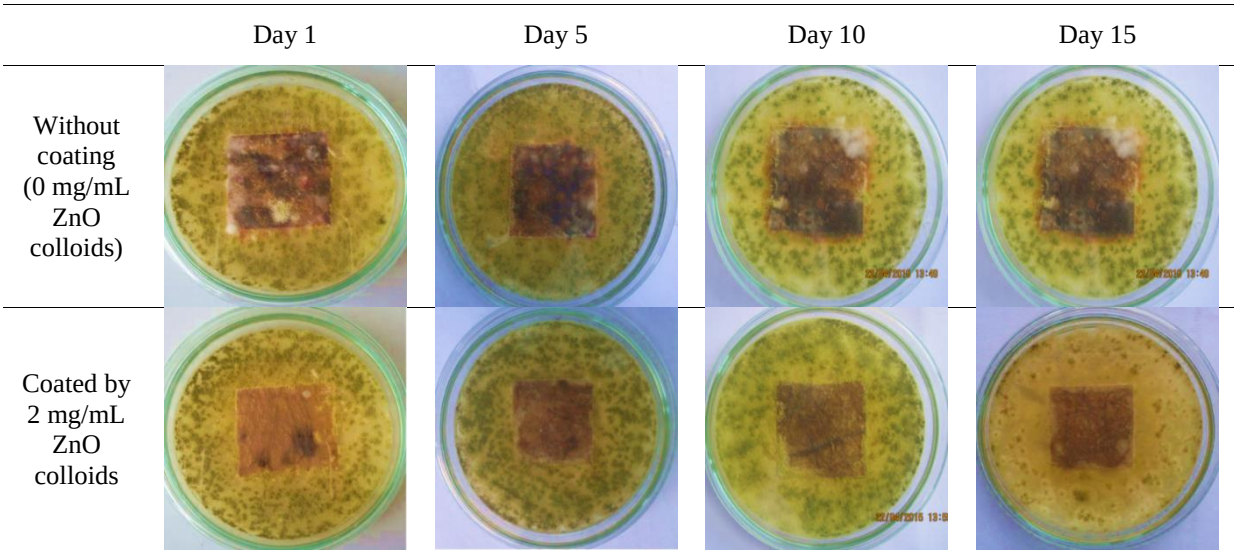

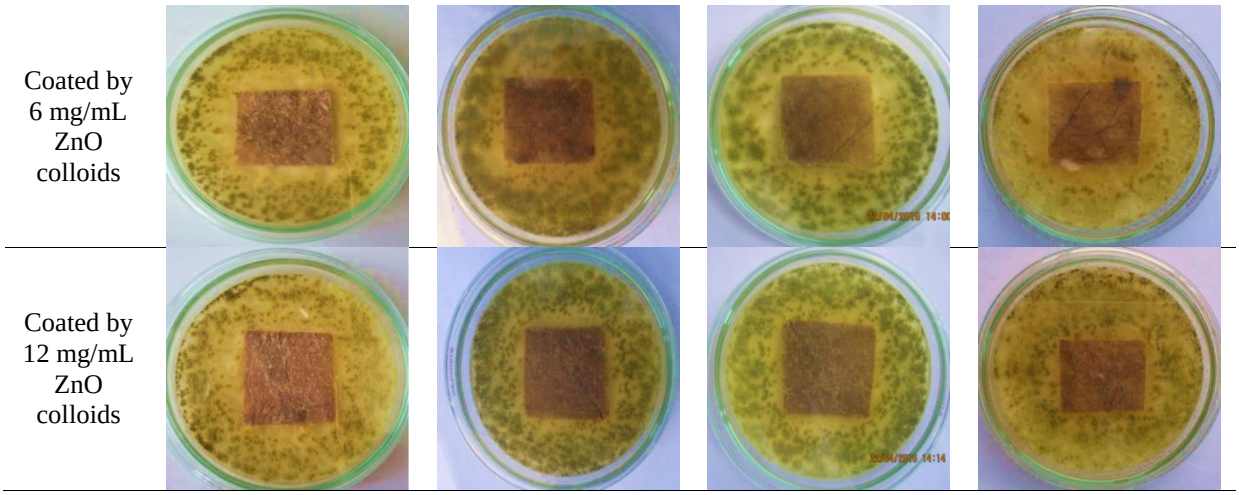

Figure 5: Comparison of antifungal mulberry papers coated by (a) 0, (b) 2, (c) 6 and (d) 12 mg/mL of ZnO dispersion

The inhibitory mechanisms of ZnO against fungi have been discussed by several researchers. For example, it has been proposed that the surface of fungal hyphae is deformed after exposure to ZnO nanoparticles. The increased production of nucleic acids and carbohydrates through the stress response in fungal hyphae leads to cell death.[7] Similarly, the rupture of the cell membrane decreases the fungal enzymatic activity.[10] In addition, the hydrogen peroxide generated from ZnO is the major contributor of antifungal activity.[24] The damage to the cell membrane directly results in the leakage of minerals, proteins and genetic materials, causing cell death.[9] Moreover, the photocatalytic activity, related to the ZnO response to visible light, has been demonstrated as an effective mechanism in antibacterial coating.[25,26]

CONCLUSION

Single-phase ZnO microclusters obtained by a cost-effective method – the calcination of Zn $(NO_3)_2{\cdot}6H_2O$ – were used to coat mulberry papers and their antifungal properties were then investigated. The variation in the calcination temperature from 600 to 800 °C did not significantly affect the morphology and the optical properties of ZnO. The ZnO dispersion with concentrations of 2, 6 and 12 mg/mL applied on mulberry papers was found to effectively inhibit the growth of *A. niger*, as evaluated during periods of up to 15 days.

ACKNOWLEDGEMENTS: This work was supported by the research project fund of Department of Physics, Faculty of Science, Thaksin University (Phatthalung Campus).

REFERENCES

1 R. F. C. Naczi and B. A. Ford, "Sedges: Uses, Diversity, and Systematics of the *Cyperaceae*" St. Louis, Missouri Botanical Garden, 2008, p. 298.
2 N. Matan, N. Mahan and S. Ketsa, *J. Appl. Microbiol*., **115**, 376 (2013).
3 A. Sirelkhatim, S. Mahmud, A. Seeni, N. H. M. Kaus, L. C. Ann *et al*., *Nano-Micro Lett*., **7**, 219 (2015).
4 S. Vlad, L. M. Gradinaru, C. Ciobanu, D. Macocinschi, D. Filip *et al*., *Cellulose Chem. Technol*., **49**, 905 (2015).
5 C. T. M. Natercia, C. S. R. Freire, C. P. Neto, A. J. D. Silvestre, J. Causio *et al*., *Colloid. Surfaces A*, **417**, 111 (2013).
6 B. Pang, J. P. Yan, L. Yao, H. Liu, J. Guan *et al*., *RSC Adv*., **6**, 9753 (2016).
7 L. He, Y. Liu, A. Mustapha and M. Lin, *Microbiol. Res*., **166**, 207 (2011).
8 J. Sawai and T. Yoshikawa, *J. Appl. Microbiol*., **96**, 803 (2004).
9 S. Gunalan, R. Sivaraja and V. Rajendran, *Prog. Nat. Sci. Mater. Int*., **22**, 693 (2012).
10 D. Sharma, J. Rajput, B. S. Kaith, M. Kaur and S. Sharma, *Thin Solid. Films*, **519**, 1224 (2010).
11 S. Vlad, C. Tanase, D. Macocinschi, C. Ciobanu, T. Balaes *et al*., *Dig. J. Nanomater. Biostruct*., **7**, 51 (2012).
12 O. M. El-Feky, E. A. Hassan, S. M. Fadel and M. L. Hassan, *J. Cult. Herit*., **15**, 165 (2014).

[13] P. Marzbani, Y. M. Afrouzi and A. Omidvar, *Maderas Cienc. Tecnol.*, **17**, 63 (2015).
[14] M. Jaisai, S. Baruah and J. Dutta, *Beilstein J. Nanotechnol.*, **3**, 684 (2012).
[15] M. Pudukudy, Z. Yaakob, R. Rajendran and T. Kandaramath, *React. Kinet. Mech. Catal.*, **112**, 527 (2014).
[16] G. P. Merceroz, R. Thierry, P. H. Jouneau, P. Ferret and G. Feuillet, *Nanotechnology*, **23**, 125702 (2012).
[17] J. Joo, B. Y. Chow, M. Prakash, E. S. Boyden and J. M. Jacobson, *Nature Mater.*, **10**, 596 (2011).
[18] C. Pholnak, C. Sirisathitkul, D. J. Harding and S. Danworaphong, *J. Optoelectron. Adv. Mater.*, **14**, 441 (2012).
[19] R. C. Pawar, D. Cho and C. S. Lee, *Curr. Appl. Phys.*, **13**, S50 (2013).
[20] C. Pholnak, C. Sirisathitkul, S. Suwanboon and D. J. Harding, *Mater. Res.*, **17**, 405 (2014).
[21] R. Shabannia, *Iran. J. Sci. Technol. Trans. A*, **40**, 19 (2016).
[22] S. K. Mishra, R. K. Srivastava and S. G. Prakash, *J. Mater. Sci.: Mater. Electron.*, **24**, 125 (2013).
[23] J. Yang, X. Li, J. Lang, L. Yang, M. Gao *et al.*, *J. Alloys Compd.*, **509**, 10025 (2011).
[24] V. Prasad, A. J. Shaikh, A. A. Kathe, D. K. Bisoyi and A. K. Verma, *J. Mater. Process. Technol.*, **210**, 1962 (2010).
[25] S. Baruah, M. Jaisai, R. Imani, M. M. Nazhad and J. Dutta, *Sci. Technol. Adv. Mater.*, **11**, 055002 (2010).
[26] P. Sathe, K. Layman, M. T. Z. Myint, S. Dobretsov, J. Richter *et al.*, *Sci. Report.*, **7**, 3624 (2016).